On the high-pressure phase stability and elastic properties of β-titanium alloys

D. Smith[a,b], O. P. J. Joris[c], A. Sankaran[c], H. E. Weekes[c], D. J. Bull[a], T. J. Prior[d], , D. Dye[c], D. Errandonea[e] & J. E Proctor[a,b,*]

[a]School of Computing, Science & Engineering, University of Salford, Salford, M5 4WT, UK

[b]Department of Physics & Mathematics, University of Hull, Hull, HU6 7RX, UK

[c]Department of Materials, Royal School of Mines, Imperial College, London, SW7 2BP, UK

[d]Department of Chemistry, University of Hull, Hull, HU6 7RX, UK

[e]Departamento di Física Aplicado – ICMUV, Universidad de Valencia, 46100 Valencia, Spain

*Author to whom correspondence should be addressed. Email: J.E.Proctor@salford.ac.uk

Abstract

We have studied the compressibility and stability of different β-titanium alloys at high pressure, including binary Ti-Mo, Ti-24Nb-4Zr-8Sn (Ti2448) and Ti-36Nb-2Ta-0.3O (*gum metal*). We observed stability of the β phase in these alloys to 40 GPa, well into the ω phase region in the P-T diagram of pure titanium. *Gum metal* was pressurised above 70 GPa and forms a phase with a crystal structure similar to the η phase of pure Ti. The bulk moduli determined for the different alloys range from 97 ± 3 GPa (Ti2448) to 124 ± 6 GPa (Ti-16.8Mo-0.13O).

Keywords: titanium; titanium alloys; biomaterials; phase stability; diamond anvil cell

Introduction

Titanium alloys are used in the aerospace industry for their high fatigue limit up to around 550 °C, in chemical plants for their corrosion resistance and in medicine due to their relative bioinertness [1]. Ti possesses various polymorphs close to ambient conditions – the stable hcp α phase, bcc β phase accessible at 900 °C [2] and hexagonal ω phase at modest high pressures; metastable at ambient conditions [3, 4]. Accessibility of solid state phase transformations, with alloying to change the relative stability of phases, enables a wide range of processing options and a myriad of microstructures – and hence properties – in conventional alloys [1]. Alloying with Mo, V, Cr, Ta and Nb stabilizes the β phase, whilst Al stabilises the α phase [5] – for instance in the widely-used alloy Ti-6Al-4V (*Ti64*) where

alloying stabilises the α phase with respect to pressure, more than doubling the α → ω transition pressure to 32GPa [6].

It is important to note that, even in nominally pure Ti, a variety of different transition pressures have been observed for the α→ω transition. The variation has been attributed to the choice of different pressure transmitting media (PTM) in different studies [3], and hence it has been suggested that the transition pressure varies depending on the hydrostaticity of the high pressure environment. However, the observed transition pressure does not appear to depend on hydrostaticity in a systematic manner (ref. [7], ref. [3] and references therein). In one study with no PTM, the transition occurred at 2.9 GPa [8], whilst in another study with no PTM the transition took place at 7.4 GPa [9]. On the other hand, the observed transition pressures in Ar [3] and He [7] are very similar (10.5 – 14.9 GPa and 10.1 – 14.6 GPa) despite He providing a far more hydrostatic environment than Ar [10].

We therefore note that the factors affecting the observed transition pressure are not limited to the hydrostaticity of the pressurising environment. In particular, all Ti samples contain some small amount of interstatial oxygen (O), which diffuses into the bulk of the Ti from the surface oxide layer. We propose that this may also have a significant effect on the α → ω transition pressure, as has been suggested as long ago as 1977 [8]. The presence of interstitial O also increases the temperature of the α → β transition at ambient pressure [11].

Recently, the properties of highly-alloyed metastable β Ti alloys, such as Ti-36Nb-2Ta-0.3O (wt. %, *gum metal*) [12] and Ti-24Nb-4Zr-8Sn-xO (wt %, Ti2448) have been explored. In these, the β phase is stabilised to room temperature, whereupon Young's moduli of ca. 50 GPa are observed [13] – compared to over 100 GPa in conventional α and α + β alloys. Since stress shielding can lead to bone resorption in biomedical implants, these low-moduli alloys are attractive [14]. Where the single-crystal moduli have been determined, it is found that the C′ shear modulus in particular can be quite low, ~16 GPa, indicating a decreasing stability against shear [15, 16]. Alloying with V and Al is avoided due to cytotoxicity [16, 17].

It is now accepted that this class of alloy forms a variety of shear-related deformation structures, including the orthorhombic α″ martensite – which can be formed through tensile [11, 15, 18] and shock [19] loading – as well as twins and stacking faults. The martensitic α″ phase is also found to be super-elastic in these alloys [18]. Super-elastic β-Ti alloys are of interest in their own right, provoking interest in the Ti-Mo system [20, 21]. Interstitial O also appears to increase the transformation temperature [11]. In addition, rather surprisingly, the ω phase appears to be produced by cold work [15] – potentially rationalised by reference to the hydrostatic stress, ca. 1 – 5 GPa, found in dislocation cores. In *Ti2448*, the

ω phase is produced by heat treatment to just 80 °C at ambient pressure [22], causing concern with regards to embrittlement.

Various methods are used to evaluate the stability of different alloys, but surprisingly little data is available measuring the stability directly by measuring phase transition pressures. This is important when considering prosthetics and orthopaedics as mechanically-induced transitions could cause embrittlement as small areas transform out of the desirably-ductile β phase. Whilst GPa pressures will not be generated in the bulk of the implant during everyday use, they can exist in the vicinity of dislocations. The only static high pressure data available to our knowledge on the effect of alloying on phase stability in Ti are studies on Ti64 [6] and Ti-15Mo-3Nb-3Al-0.2Si (wt%, *Ti-β-21S*) [23]. Here, we have therefore examined the phase stability of a range of β-stabilised Ti alloys under quasi-hydrostatic compression and performed in-situ synchrotron X-ray diffraction (XRD) on these alloys in diamond anvil high pressure cells (DACs).

Methods

Samples of β-titanium alloys: Ti-13.5Mo-0.26O, Ti-13.5Mo-0.40O and Ti-16.8Mo-0.13O (wt. %) were prepared by arc melting pure master elements – using TiO to add O – under argon, homogenising and hot rolling [21]. We record no presence of any α-Ti peaks in our Ti-Mo alloys, where typically a minimum of 15 wt. % Mo has been required to produce an alloy consisting only of the β phase, or 10 wt. % in the quenched condition [1, 16, 24]. Ti-24Nb-4Zr-8Sn (*Ti2448*) samples were prepared at the Chinese Academy of Science Institute of Metal Research by arc melting alloying constituents with a Ti-Sn master and hot rolling [22]. Ti-36Nb-2Ta-0.3O (*gum metal*) was synthesised from pure elements by plasma arc melting and hot rolled into a plate. Powders were prepared by grinding and magnetically separated from any file debris. A powder of commercially-pure (CP) titanium (Grade 1, Timet Corporation; Henderson, NV) was used for a control experiment. In all cases, the composition of samples was verified by chemical analysis with inductively-coupled plasma atomic emission spectroscopy (Incotest, LSM) for the transition metals and inert gas fusion (LECO) for O – see Table 1.

	wt. %						at. %					
	Mo	Nb	Ta	Zr	Sn	O	Mo	Nb	Ta	Zr	Sn	O
gum metal [25]		36.2	1.97	3.16		0.26		23.3	0.65	2.07		0.97
Ti2448 [26]		21.6		3.82	7.25	0.08		13.3		2.4	3.5	0.3
Ti-13.5Mo-0.26O [21]	13.51					0.27	7.2					0.86
Ti-13.5Mo-0.40O [21]	13.55					0.40	7.2					1.27
Ti-16.8Mo-0.13O [21]	16.8					0.13	9.1					0.42

Table 1. Measured bulk compositions of the alloys examined, measured by ICP-OES (transition elements) and inert gas fusion / LECO (O) at LSM and Incotest.

High pressure experiments were prepared by first equipping DACs with diamonds having polished culets ranging from 250-450 μm. Stainless steel or rhenium gaskets were pre-indented from an initial thickness of 200 μm to a thickness of 25-50 μm and a sample chamber drilled in the indentation using electric discharge machining (EDM). Small amounts of the powdered samples were placed in the sample chamber and cryogenic nitrogen added to serve as a pressure transmitting medium (PTM). X-ray diffraction (XRD) patterns were collected at Diamond Light Source using monochromatic X-rays (λ = 0.42460 and 0.41336 Å) and a MAR345 image plate. The FIT2D software package was used to calibrate diffraction parameters and integrate the two-dimensional diffraction images to one-dimensional intensity-versus-2θ plots. Structural analysis was performed with GSAS and PowderCell software. Pressure was determined by measuring the fluorescence peak shift from a ruby chip placed inside the sample chamber. All experiments were carried out at room temperature.

Results

To characterize any effects that the nitrogen PTM may have on phase stability, the ambient α phase CP Ti powder was pressurised, whereupon we observed a complete transition between the α and ω phases commencing at 6.3 GPa and completing by 9.4 GPa, shown in Fig. 1.

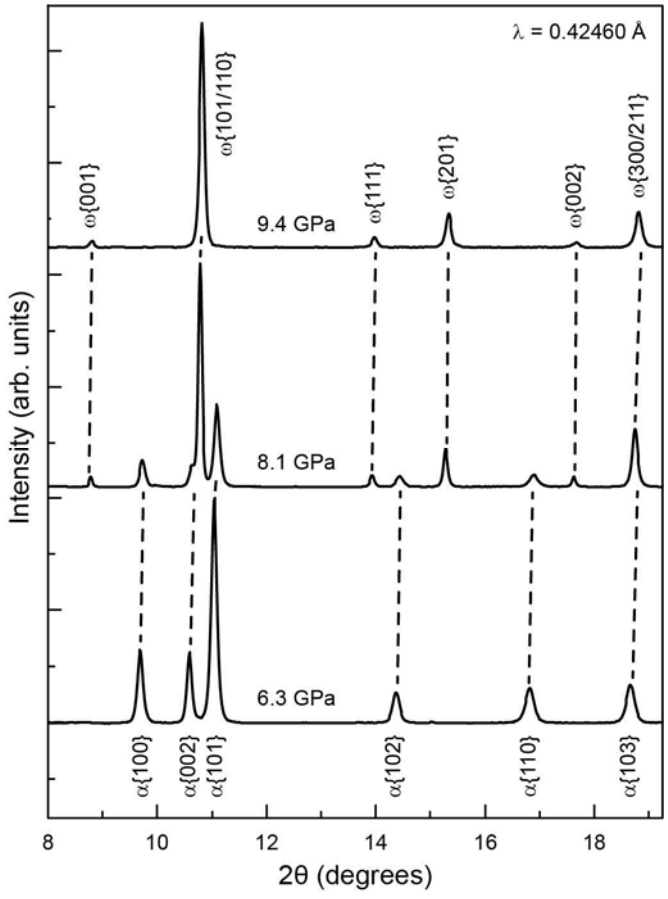

Fig. 1. Integrated XRD patterns displaying the α → ω transition in commercially pure (CP) Ti under quasi-hydrostatic compression in a nitrogen PTM, commencing at 6.3 and ending by 9.4 GPa, Bragg peaks from both phases are indexed.

The β-stabilised alloys studied were compressed to pressures shown in Table 2 and their XRD patterns collected upon pressure increase only. Fig. 2 shows the XRD patterns of Ti-13.5Mo-0.26O (wt. %), Ti-13.5Mo-0.40O (wt. %) and Ti2448 at 40.4, 45.7 and 40.8 GPa respectively, demonstrating stability within the β phase throughout the entire compression sequence.

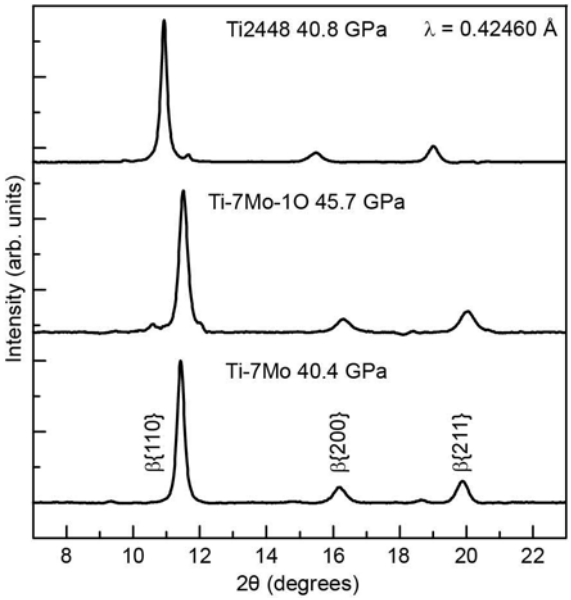

Fig. 2. Integrated XRD patterns of Ti-7Mo, Ti-7Mo-1O and Ti2448 at maximum pressure, indexed with Bragg reflections from the β phase. No emergence of secondary phases was observed in these alloys at high pressure.

From the XRD patterns we determined the molar volumes of each alloy under compression by structural refinement in GSAS. Pressure-volume equations of state were fitted in OriginPro 9.0 with the parameters shown in Table 2. We opt for the Birch-Murnaghan (BM) equation of state (EOS) with a third-order truncation (Eq. 1) as well as a second-order truncation (B_0' fixed at 4). The fits using the third-order truncation are shown in Fig. 3a and those with the second order truncation in Fig. 3b.

$$P(V) = \frac{3B_0}{2}\left[\left(\frac{V_0}{V}\right)^{\frac{7}{3}} - \left(\frac{V_0}{V}\right)^{\frac{5}{3}}\right]\left[1 + \frac{3}{4}[B_0' - 4]\left[\left(\frac{V_0}{V}\right)^{\frac{2}{3}} - 1\right]\right] \quad (1)$$

We use fitted parameters from the second-order Birch-Murnaghan fitting for direct comparison of volume evolution with pressure between alloys since bulk compressibility and its pressure derivative are correlated [27], rendering direct comparison between fitting parameters in the third order EOS not reliable. Typical reduced χ^2 values for each fit are around 1.3 for third-order equations of state and 2.3 for second-order. For comparison, we include also in Table 2 B_0 and B_0' for the pure phases of Ti and Ti-β-21S.

			3rd-order		2nd-order	
	P_{max} (GPa)	V_0 (cm^3 mol^{-1})	B_0 (GPa)	B_0'	B_0 (GPa)	Reference
Ti-13.5Mo-0.26O	40.4	10.38	98 ± 7	5.3 ± 0.8	111 ± 2	This study
Ti-13.5Mo-0.40O	45.7	10.42	141 ± 6	2.3 ± 0.3	113 ± 2	This study
Ti-17Mo-0.13O	10.5	10.42	--[a]	--[a]	124 ± 6	This study
Ti2448	40.8	10.82	55 ± 9	10.5 ± 2.5	97 ± 3	This study (V_0 from ref. [21])
gum metal[b]	72.4	10.78	111 ± 4	4.3 ± 0.3	117 ± 1	This study
α-Ti		10.66	117 ± 9	3.9 ± 0.4		[3]
ω-Ti		10.48	138 ± 10	3.8 ± 0.5		[3]
β-Ti		10.72	96	3.1		[7] (Rydberg-Vinet EOS)
Ti-β-21S	71	10.49	109.7	3.698		[23]

[a]Insufficient data collected for alloy to allow a third-order Birch-Murnaghan EOS to be fitted.

[b]With 50.7 GPa outlying point included, B_0 = 118 ± 10 GPa, B_0' = 3.8 ± 0.6 (third-order EOS) and B_0 = 114 ± 2 GPa (second-order EOS).

Table 2. Bulk moduli and their pressure derivatives for presented alloys according to third- and second-order Birch-Murnaghan EOS (except where otherwise stated).

Gum metal was pressurised to 72.4 GPa and remained in the β phase to around 70 GPa, its β phase EOS is plotted in Fig. 2. One outlying data point was identified at 50.7 GPa, the omission of which drastically improved the goodness of the EOS fit (reduced χ^2 value reduced from ca. 10 to 2 upon omission). Standard error in the lattice parameters from structural refinement equates to an average 0.2% error in molar volumes. Such uncertainties are too small to include in Fig. 3 as error bars.

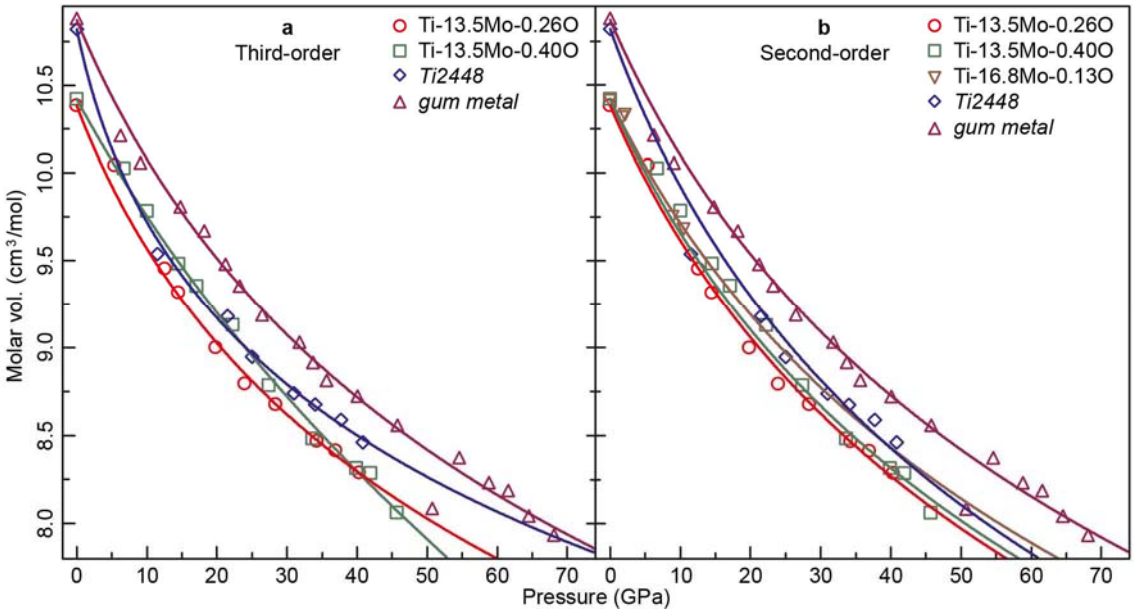

Fig. 3. (colour online) Pressure-volume evolution for alloys in the β phase fitted with (a) Third-order Birch-Murnaghan and (b) second-order Birch Murnaghan EOS. Error bars are comparable in size to symbols and thus neglected.

At 72.4 GPa, we observe emergence of a secondary phase in *gum metal*. Pure Ti has two orthorhombic phases occurring above 1 Mbar [28]: the γ phase commencing at 116 GPa [29] and the δ phase commencing at 140 GPa [9], but the reported structure of both of these phases should lead to reflections at higher angles which are not observed here. Ref. [30] have seen a distorted phase – termed the η phase – emerging in Ti upon laser heating to 1200–1300 K at 80 GPa, which we consider the most likely candidate structure for the transition observed in *gum metal*, Fig. 4a shows the location of β and η Bragg reflections after Le Bail refinement [*Fmmm*, space group no. 69, a = 4.0061(9) Å, b = 4.4040 (9) Å and c = 3.0199(9) Å].

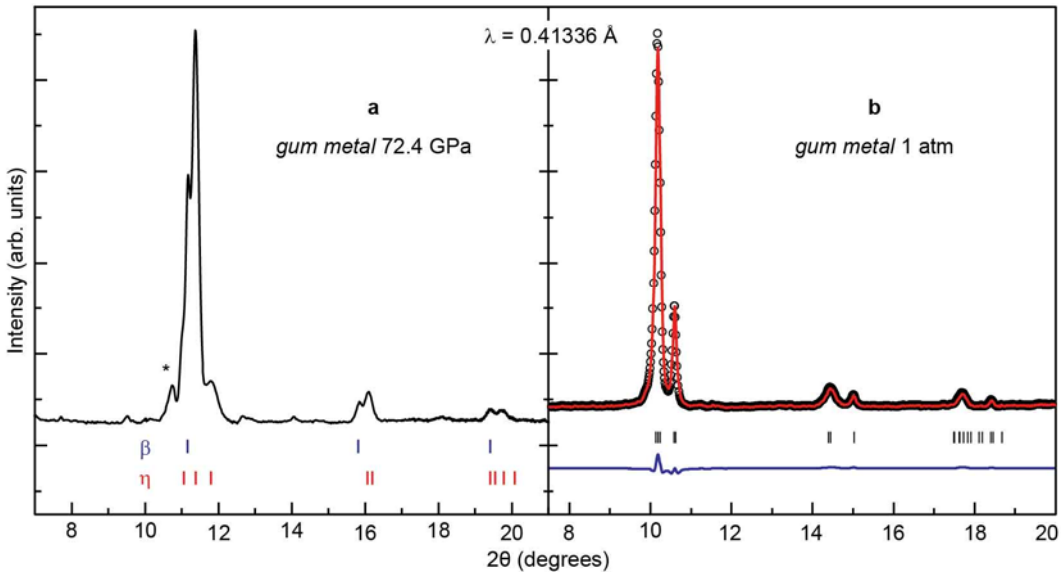

Fig. 4. (colour online) (a) XRD pattern of *gum metal* at 72.4 GPa. Tick marks show peak positions from β phase η phase, asterisk marks peak due to ruby. (b) XRD pattern of recovered *gum metal*. Open circles are data, red line is refinement in PowderCell, tick marks show predicted reflection locations of the triclinic structure and blue line is fit residual.

Fig. 4b shows the XRD pattern of *gum metal* following gradual pressure release from 72.4 GPa to ambient pressure. By reducing the symmetry of this structure using group-subgroup relationships available in PowderCell, we could describe the XRD pattern of our recovered sample by a triclinic structure ($P\bar{1}$ space group no. 2) which we will call β′. Our β′ phase has one Ti atom per formula unit at the Wyckoff position 1a (0, 0, 0), lattice parameters a = 2.8212(9), b = 2.7358(9), and c = 3.2903(9) Å, angles α = 124.86(9)°, β = 124.35(9)° and γ = 72.92(9)°. It is important not to confuse β′, our distorted bcc structure, with the metastable bcc phase from Ref. [30], which was named β′ for being isostructural with the β phase.

Discussion

In this work, we have conducted a wide-ranging study of the effect of alloying on the compressibility and phase stability of β-Ti (see Table 2) a wide variety of compressibilities and EOS curves are attainable by alloying. In general, we observe compressibilities which are between that of pure β-Ti and pure α-Ti. Whilst β-Ti has a bulk modulus (with third order truncation) of 96 GPa, production of the β phase by alloying can reduce the bulk modulus to as low as 55 GPa in the case of Ti2448. Whilst *Ti2448* is by far the most compressible alloy at ambient conditions it becomes the least compressible above *ca.* 20 GPa due to the high value of B_0' when the third order truncation is used (10.5). The use of a second order truncation leads to a fitted EOS that slightly underestimates the volume at the highest

pressures studied. The ambient compressibility of *gum metal* measured here is found to be close to that for similar super-elastic alloys studied using acoustic resonance in Ref. [31] containing 0.36 wt. % O.

We note, particularly with reference to our data on Ti-16.8Mo-0.13O, that adding Mo increases B_0 (relative to other β-Ti alloys such as *gum metal* and *Ti2448*) and attribute this to the relative hardness of Mo (B_o = 268 GPa [32]). Although little data was taken on the high-Mo alloy, its enhanced B_0 compared with other alloys tentatively suggests a tailorable compressibility in simple Ti-Mo binary alloys as a function of stoichiometry. However, the heightened Mo content potentially causes potential problems with respect to medical applications, where stabilising in the β phase is desirable in order to reduce B_0 compared to α-Ti to better match the elastic properties of bone.

In our control experiment on pure Ti, we observe a relatively low pressure for the α → ω transition compared to those observed by other authors, despite using a nitrogen PTM which gives a compressive atmosphere comparable to that of Ne or He below 10 GPa [10]. The transition pressure observed corresponds most closely with that observed in Ar [3], which has a hydrostaticity similar to nitrogen only beyond 10 GPa [10]. We acknowledge the role of interstitial oxygen in altering transition pressure, contamination with oxygen is known to have the effect of stabilising the α phase, and that the lack of O in our high-purity Ti sample would also have the effect of lowering the α → ω transition pressure.

On the other hand, we note that deliberate addition of oxygen appears to have little effect on the stability with respect to pressure of alloys which are already in the β phase at ambient conditions; both Ti-13.5Mo-0.26O and Ti-13.5Mo-0.40O were stable to their highest studied pressure with no secondary phases emerging (Figure 2) and, for a second-order EOS (B_0' fixed at 4), their compressibilities are comparable within error. This finding reinforces the conclusions of a recent *ab initio* study on binary Ti alloys Ti-*X* (*X* = Nb, Zr and Sn – known β-stabilisers) and on *Ti2448*, which suggest O as having only a small effect on elastic properties in these alloys [33]. For third-order Birch-Murnaghan EOS, the bulk modulus obtained from our measurements is significantly higher for Ti-13.5Mo-0.40O than for Ti-13.5Mo-0.26O (Table 2), but it is likely that this is correlated to some extent with the value of B_0' which is much lower for Ti-13.5Mo-0.4O. We suggest, then, that the naturally-occurring O expected from industrialised alloying and the oxides expected to form in biological environments [17] have little effect on the elastic properties of Ti-Mo binary alloys.

Generally, the β-Ti alloys synthesised here exhibit extremely good stability against pressure-induced transitions to other phases. Binary Ti-Mo alloys showed stability within the β phase to 40.4 – 45.7 GPa and it will be interesting to compare against the stability of other binary β-Ti alloys in future compression experiments, in particular for similar Ti-Nb, since the β-stabilising properties of Mo surpass that of Nb due to its additional valence electron [34]. Only in the case of *gum metal*, where we

compressed to extremely high strain rates, did we observe any transitions to different phases. *In situ* XRD measurements at 72 GPa show that *gum metal* transforms to a structure similar to that reported for the η phase of pure Ti [30]. That the observed high pressure phase appears to be isostructural to a phase previously observed only at high pressure and high temperature in pure Ti is not surprising, since the β phase – into which *gum metal* is stabilised through alloying – is itself a high temperature phase in pure Ti. Upon pressure release, *gum metal* transformed relaxed into a triclinic distorted bcc structure which we call β′, not previously observed in Ti or Ti alloys. That *gum metal* did not relax into the bcc β phase and that it formed a low-symmetry phase at high pressure are likely consequences of the non-hydrostatic nature of the nitrogen pressurising atmosphere at 72 GPa, hindering the ability of the lattice to restructure efficiently into its high *P* phase. The low-symmetry phase found upon pressure release is potentially a metastable phase at an incomplete stage of a structural transformation between the β phase and some high-*P* phase which has been quenched by a fast downstroke in pressure. Recently, Ref [35] have seen theoretical evidence for a metastable orthorhombic structure occurring during the α → ω transformation in pure Ti, but do not evaluate its potential recovery to ambient P.

Conclusions

We report the room-temperature compression and equations of state for a range of Ti alloys stabilised in the bcc β phase, which show good phase stability within the pressure ranges studied. Only Ti-36Nb-2Ta-0.3O (*gum metal*) exhibits any secondary phases, but at extremely high levels of compression. Although the presence of oxygen can have significant effects on the relative stability with respect to pressure of the various phases in pure Ti, we have found that the element has little effect on the ability of Mo to stabilise Ti in the β phase, and surprisingly little effect on the elastic properties of Ti-Mo binary alloys. The high pressure phase observed in *gum metal* – structurally similar to a high *P*-*T* phase in pure Ti – may suggest that more extensive alloying and treatment could see further Ti phases stabilised to ambient conditions.

Acknowledgements

X-ray diffraction data was collected at beamline I15 at Diamond Light Source, UK (beamtime EE8724). The authors would like to thank Annette Kleppe and Heribert Wilhelm for assistance at the synchrotron and James Coakley of Northwestern University for helpful discussion. D.E. thanks the financial support of Spanish MINECO under Grants No. MAT2013-46649-C04-01/02/03 and No. MAT2015-71070-REDC (MALTA Consolider). Provision of material by Prof Rui Yang of the Chinese Academy of Science Institute of Metal Research, Shenyang, China, is gratefully acknowledged, as is funding by EPSRC [grant EP/H004882/1].

References

[1] G. Lutjering and J. C. Williams, Titanium, Springer-Verlag, Berlin Heidenberg, 2007.

[2] J. Zhang, Y. Zhao, R. S. Hixson, G. T. Gray III, L. Wang, W. Utsumi, S. Hiroyuki, H. Takanori, Experimental constraints on the phase diagram of titanium metal, J. Phys. Chem. Solids 69 (2008) 2559-2563.

[3] D. Errandonea, Y. Meng, M. Somayazulu, D. Häusermann, Pressure-induced α → ω transition in titanium metal: a systematic study of the effects of uniaxial stress, Physica B 355 (2005) 116-125.

[4] E. Yu. Tonkov, E. G. Ponyatovsky, Phase Transformations of the Elements Under High Pressure, CRC Press, Boca Raton, 2004.

[5] R. G. Hennig, D. R. Trinkle, J. Bouchet, S. G. Srinivasan, R. C. Albers, J. W. Wilkins, Impurities block the α to ω martensitic transformation in titanium, Nat. Mater. 4 (2005) 129-133.

[6] S. G. Macleod, B. E. Tegner, H. Cynn, W. J. Evans, J. E. Proctor, M. I. McMahon, G. J. Ackland, Experimental and theoretical study of Ti-6Al-4V to 220 GPa, Phys. Rev. B 85 (2012) 224202.

[7] A. Dewaele, V. Stutzmann, J. Bouchet, F. Bottin, F. Occelli, M. Mezouar, High pressure-temperature phase diagram and equation of state of titanium, Phys. Rev. B 91 (2015) 134108.

[8] Y. K. Vohra, S. K. Sikka, S. N. Vaidya and R. Chidambaram, Impurity effects and reaction kinetics of the pressure-induced α→ω transformation in Ti, J. Phys. Chem. Sol. **38**, 1293 (1977)

[9] Y. Akahama, H. Kawamura, T. Le Bihan, New δ (Distorted-bcc) Titanium to 220 GPa, Phys. Rev. Lett. 87 (2001) 275503.

[10] S Klotz, J.-C. Chervin, P Munsch, G. Le Marchand, Hydrostatic limits of 11 pressure transmitting media, J. Phys. D: Appl. Phys 42 (2009) 075413.

[11] E. G. Obbard, Y. L. Hao, R. J. Talling, S. J. Li, Y. W. Zhang, D. Dye, R. Yang, The effect of oxygen on α″ martensite and superelasticity in Ti–24Nb–4Zr–8Sn, Acta Mater. 59 (2011) 112-125.

[12] T. Saito, T. Furuta, J.-H. Hwang, S. Kuramoto, K. Nishino, N. Suzuki, R. Chen, A. Yamada, Y. Ito, Y. Seno, T. Nonaka, H. Ikehata, N. Nagasako, C. Iwamoto, Y. Ikuhara, T. Sakuma, Multifunctional Alloys Obtained via a Dislocation-Free Plastic Deformation Mechanism, Science 300 (2003) 464-467.

[13] R. J. Talling, R. J. Dashwood, M. Jackson, D. Dye, Determination of ($C_{11} - C_{12}$) in Ti–36Nb–2Ta–3Zr–0.3O (wt. %) (Gum metal), Acta Mater. 57 (2008) 1188-1198.

[14] Z. Guo, J. Fu, Y. Q. Zhang, Y. Y. Hu, Z. G. Wu, L. Shi, M. Sha, S. J. Li, Y. L. Hao, R. Yang, Early effect of Ti–24Nb–4Zr–7.9Sn intramedullary nails on fractured bone, Mater. Sci. Eng. C 29 (2009) 963-968.

[15] R. J. Talling, R. J. Dashwood, M. Jackson, D. Dye, On the mechanism of superelasticity in Gum metal, Acta Mater. 57 (2009) 1188-1198.

[16] N. T. C. Oliveira, G. Aleixo, R. Caram, A. C. Guastaldi, Development of Ti–Mo alloys for biomedical applications: Microstructure and electrochemical characterization, Mater. Sci. Eng. A 452-453 (2007) 727-731.

[17] N. T. C. Oliveira, A. C. Guastaldi, Electrochemical stability and corrosion resistance of Ti–Mo alloys for biomedical applications, Acta Biomater. 5 (2008) 399-405.

[18] H. Y. Kim, Y. Ikehara, J. I. Kim, H. Mosoda and S. Miyazaki, Martensitic transformation, shape memory effect and superelasticity of Ti–Nb binary alloys, Acta Mater. 54 (2006) 2419-2429.

[19] Y. Ren, F. Wang, C. Tan, S. Wang, X. Yu, J. Jiang, H. Cai, Effect of shock-induced martensite transformation on the postshock mechanical response of metastable β titanium alloys, J. Alloy. Compd. 578 (2013) 547-552.

[20] F. Sun, F. Prima, T. Gloriant, High-strength nanostructured Ti–12Mo alloy from ductile metastable beta state precursor, Mat. Sci. Eng. A 527 (2010) 4262-4269.

[21] O. Joris, Diffraction Experiments on Superelastic Beta Titanium Alloys [dissertation], Imperial College, London, 2015.

[22] J. Coakley, K. M. Rahman, V. A. Vorontsov, M. Ohnuma, D. Dye, Effect of precipitation on mechanical properties in the β-Ti alloy Ti–24Nb–4Zr–8Sn, Mat. Sci. Eng. A. – Struct. 655 (2016) 399-407.

[23] N. Velisavljevic, G. N. Chesnut, Direct hcp→bcc structural phase transition observed in titanium alloy at high pressure, Appl. Phys. Lett. 91 (2007) 101906.

[24] Y.-Y. Chen, L.-J. Xu, Z.-G. Liu, F.-T. Kong, Z.-Y. Chen, Microstructures and properties of titanium alloys Ti-Mo for dental use, Trans. Nonferrous Met. Soc. China 16 (2006) 824-828.

[25] J. Coakley, V. A. Vorontsov, K. C. Littrell, R. K. Heenan, M. Ohnumad, N. G. Jonese, D. Dye, Nanoprecipitation in a beta-titanium alloy, J. Alloy. Compd. **623**, 146 (2015)

[26] J. Coakley, D. Isheima, A. Radeckad, D. Dye, H. J. Stone, D. N. Seidman, Microstructural evolution in a superelastic metastable beta-Ti alloy, Scripta Mater. **128**, 87 (2016)

[27] R. J. Angel, Equations of state, Rev. Mineral. Geochem. 41 (2000) 35-59.

[28] A. L. Kutepov, S. G. Kutepova, Crystal structures of Ti under high pressure: Theory, Phys. Rev. B 67 (2003) 132102.

[29] Y. K. Vohra, P. T. Spencer, Novel γ-Phase of Titanium Metal at Megabar Pressures, Phys. Rev. Lett. 86 (2001) 3068-3071.

[30] R. Ahuja, L. Dubrovinsky, N. Dubrovinskaia, J. M. O. Guillen, M. Mattesini, B. Johansson, T. Le Bihan, Titanium metal at high pressure: Synchrotron experiments and *ab initio* calculations, Phys. Rev. B 69 (2004) 184102.

[31] M. Tane, T. Nanako, S. Kuramoto, M. Hara, M. Niinomi, N. Takesue, T. Yano, H. Nakajima, Low Young's modulus in Ti–Nb–Ta–Zr–O alloys: Cold working and oxygen effects, Acta Mater. 91 (2011) 6975-6988.

[32] Y. Zhao, A. C. Lawson, J. Zhang, B. I. Bennett, R. B. Von Dreele, Thermoelastic equation of state of molybdenum, Phys. Rev. B 62 (2000) 8766-8776.

[33] J. H. Dai, Y. Song, W. Li, R. Yang, L. Vitos, Influence of alloying elements Nb, Zr, Sn, and oxygen on structural stability and elastic properties of the Ti2448 alloy, Phys. Rev. B 89 (2014) 014103.

[34] Q. Yao, J. Sun, H. Xing, W.-Y. Guo, Influence of Nb and Mo contents on the phase stability and elastic properties of β-typ Ti-X alloys, Trans. Nonferrous Met. Soc. China 17 (2007) 1417-1421.

[33] N. A. Zarkevich, D. D. Johnson, Titanium α-ω phase transformation pathway and a predicted metastable structure, Phys. Rev. B 93 (2016) 020104.